RSC Advances

PAPER

View Article Online
View Journal | View Issue

Cite this: *RSC Adv.*, 2017, **7**, 54789

Nickel containing ionic liquid based ordered nanoporous organosilica: a powerful and recoverable catalyst for synthesis of polyhydroquinolines

Dawood Elhamifar, *[a] Hamideh Khanmohammadi[a] and Davar Elhamifar[bc]

Received 28th September 2017
Accepted 22nd November 2017

DOI: 10.1039/c7ra10758g

rsc.li/rsc-advances

A novel nickel containing alkyl-imidazolium ionic liquid based ordered mesoporous organosilica (Ni@IL-OMO) is prepared, characterized and applied as an efficient nanocatalyst in the one-pot synthesis of polyhydroquinolines through the Hantzsch reaction. The Ni@IL-OMO was prepared *via* immobilization of nickel chloride on IL-OMO at room temperature. This was characterized using transmission electron microscopy (TEM), FTIR-spectroscopy, nitrogen adsorption–desorption analysis, scanning electron microscopy (SEM) and energy-dispersive X-ray (EDX) spectroscopy. The polyhydroquinolines were obtained in high to excellent yield and selectivity in the presence of a low loading of Ni@IL-OMO with short reaction times. This catalyst was recovered and reused several times while keeping its efficiency under the applied conditions. The recovered catalyst was analyzed by TEM to study its structural stability during reaction process.

1. Introduction

The use of ordered mesoporous organosilicas (OMOs) as supports in organic transformations is a valuable concept among chemists due to the high surface area, excellent stability and good selectivity of these materials.[1–3] Especially, OMO-supported transition metals are more interesting owing to their widespread catalytic applications in several organic processes such as C–C bond formation.[3–6] Among these, metal containing periodic mesoporous organosilicas (M@PMOs) are more attractive due to the advantages of PMOs such as high lipophilicity, high thermal and mechanical stability, and easy diffusion of organic substrates in the mesochannels of these noble materials.[7,8] M@PMOs are prepared *via* impregnation of metallic salts with PMO nanomaterials and/or by simultaneous hydrolysis and condensation of metal/ligand complexes with PMO precursors under acidic or basic conditions.[7–14] Addressing some of these issues in the context of green manufacturing, several M@PMOs such as V@PMO, Cu@PMO,[7,15] Co@PMO,[7,16] Pd@PMO,[17] Rh@PMO,[18] Ru@PMO,[7,17b,18] Au@PMO,[7,17b] Mo@PMO,[19] Fe@PMO,[20] Sn@PMO,[7,15b] and Mn@PMO[7] have been prepared and applied as effective nanocatalysts in a number of organic transformations. More recently we have also prepared some ionic liquid based periodic mesoporous organosilica supported metal catalysts and studied their applications in a set of different organic processes.[21–24] These showed highly performance and stability under applied reaction conditions.

On the other hand, since discover of the Hantzsch reaction in the organic synthesis, many strategies have been developed for this important process due to its key role in the formation of biologically active and pharmacology useful compounds.[25–28] This reaction usually is performed *via* one-pot condensation of aldehydes, alkylacetoacetates and amines in the presence of both Lewis and Brønsted acid catalysts.[25–27] To date a lot of catalysts such as TMSI, $Yb(OTf)_3$, cerium(IV) ammonium nitrate, Bu_4NHSO_4, ionic liquids, bismuth(III) bromide and boronic acids have been reported for this process under homogeneous conditions.[29–36] However, due to problems concerted to homogeneous catalytic systems such as separation and purification of desired products and catalyst recovery, a lot of heterogeneous catalysts with advantages of easy recoverability and reusability have been recently used for the production of polyhydroquinolines *via* Hantzsch reaction.[37–48] Some of developed heterogeneous systems include supported metallic and organic catalysts on the surfaces of polymer, silica, carbon and alumina.[37–48] In continuous of aforementioned studies and according to importance of PMOs in catalytic processes,[49–51] herein, for the first time the nickel chloride is immobilized onto/into an ionic liquid based ordered mesoporous organosilica to prepare a novel nanocatalyst named Ni@PMO-IL. This catalyst was easily and successfully prepared at room temperature in DMSO solvent *via* impregnation method (Scheme 1). The

[a]*Department of Chemistry, Yasouj University, Yasouj, 75918-74831, Iran. E-mail: d.elhamifar@yu.ac.ir*
[b]*Department of Chemical Engineering, Isfahan University, Isfahan, Iran*
[c]*Mehr Petrochemical Company, Phase 2 of PSEEZ, Assaluyeh, Bushehr, Iran*

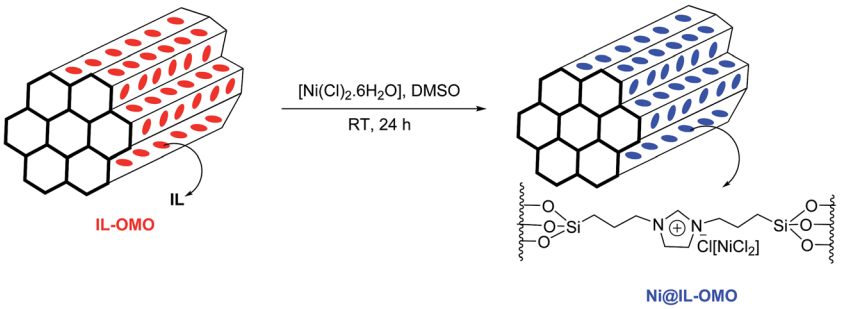

Scheme 1 Preparation of Ni@IL-OMO nanocatalyst.

Ni@PMO-IL catalyst was characterized using several techniques including TEM, nitrogen adsorption–desorption analysis, FT-IR-spectroscopy, SEM and EDX. The catalytic performance of Ni@PMO-IL was developed in the one-pot Hantzsch synthesis of different polyhydroquinolines. The study showed that the catalyst is very active in the preparation of a set of different polyhydroquinoline derivatives under solvent-free media as well as it is highly recoverable and stable under applied reaction conditions.

2. Experimental section

2.1. Preparation of Ni@IL-OMO nanocatalyst

Firstly, ionic liquid based mesoporous organosilica (IL-OMO) was prepared according to our recent reported procedure with a slight modification.[21–24] The IL-OMO was then used as support material as following: typically, 1 g of IL-OMO was added into DMSO (20 mL) and stirred at room temperature. After uniform distribution of IL-OMO, a DMSO solution of $NiCl_2 \cdot 6H_2O$ (2 mmol) was added to the reaction vessel and stirred at room temperature for 24 h. After that, the reaction mixture was filtered and washed completely with DMSO to remove unreacted nickel chloride complex. The obtained solid was then dried at 70 °C for 12 h to deliver a powder material called Ni@IL-OMO. The loading of the nickel was obtained to be 0.6 mmol g^{-1} by the means of the Ni-content obtained from inductively coupled plasma/optical emission spectroscopy (ICP-OES).

2.2. Synthesis of Hantzsch products in the presence of Ni@IL-OMO nanocatalyst

For this, aldehyde (1 mmol), dimedone (1 mmol), ethyl/methylacetoacetate (1 mmol) and ammonium acetate (1.5 mmol) were mixed in a reaction vessel and 0.5 mol percent of Ni@IL-OMO nanocatalyst was added to the mixture. This was stirred at 70 °C without solvent for an appropriate time indicated in Table 2. After the reaction was completed, it was stopped and hot ethanol (10 mL) was added. The obtained mixture was hotly filtered to remove heterogeneous Ni-based catalyst. Then, some ice species were added into filtrate to precipitate or crystallize of desired crude products. The pure products were obtained after recrystallization of crude ones in EtOH.

2.3. Procedure for the recovery of Ni@IL-OMO in the Hantzsch reaction

To do this, the reaction of benzaldehyde, dimedone, ethyl-acetoacetate and ammonium acetate was selected as a test model. After the reaction was completed in the presence of catalyst, hot ethanol (10 mL) was added and the obtained mixture was hotly filtered. The catalyst was washed carefully with ethanol and dried at 70 °C. The recovered catalyst was reused in another reaction charged with starting materials in the same amounts as the first run. These steps were repeated several times and it was observed that the catalyst could be recovered and reused at least 9 times with keeping its efficiency.

2.4. Procedure for the hot filtration test

This test was also performed on the condensation reaction of benzaldehyde, dimedone, ethylacetoacetate and ammonium acetate in the presence of Ni@IL-OMO. After about 40 mol% of reaction was completed, it was stopped and 10 mL of hot EtOH was added. This was filtered to remove heterogeneous catalyst. The solvent of filtrate was removed and the residue was allowed to continue under standard reaction as above. Interestingly, after about 2 h, only a little conversion (<5%) was observed indicting the catalyst operates in a heterogeneous pathway.

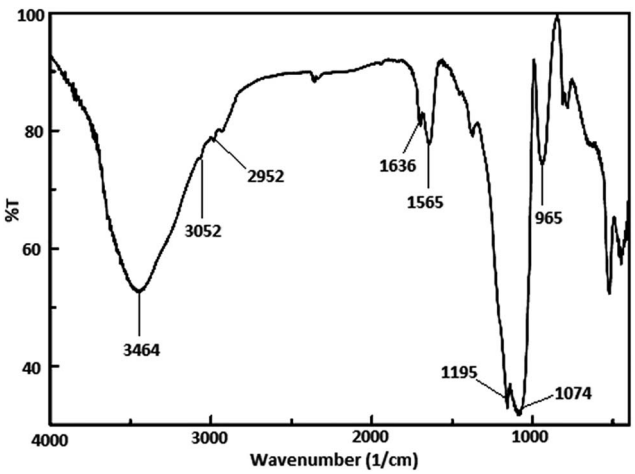

Fig. 1 FTIR spectrum of Ni@IL-OMO nanocatalyst.

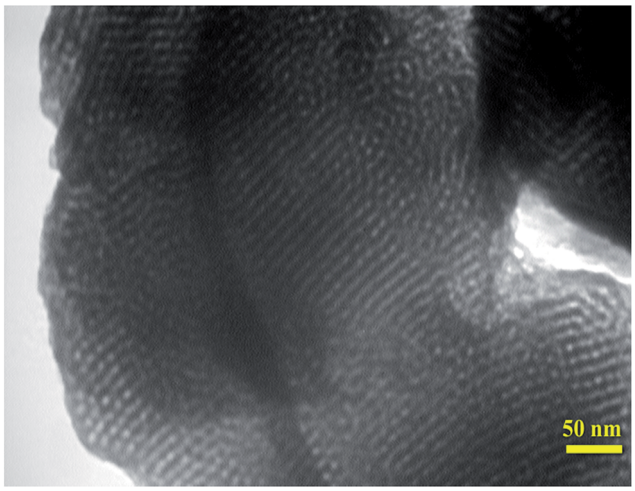

Fig. 2 TEM image of Ni@IL-OMO nanocatalyst.

3. Results and discussion

The nickel-containing ionic liquid based ordered mesoporous organosilica was prepared by treatment of $Ni(Cl)_2 \cdot 6H_2O$ with IL-OMO in DMSO at room temperature (Scheme 1).

The Ni@IL-OMO was firstly characterized by FTIR-spectroscopy to show the presence of expected organic functional groups in the material framework (Fig. 1). The strong signals cleared at 1074 and 965 cm^{-1} are assigned to asymmetric and symmetric stretching vibrations of Si–O–Si bonds. The peaks of 2952 and 3052 cm^{-1} are assigned, respectively, to aliphatic and aromatic C–H stretching vibrations of the propyl-imidazolium moieties. The C=N and C=C stretching vibrations of imidazolium ring are observed, respectively, at 1636 and 1565 cm^{-1}. The broad peak cleared about 3392 cm^{-1} is also attributed to O–H stretching vibration of material surface. Moreover, the other signals observed at 700–900 cm^{-1} are corresponded to stretching vibration of C–Si bonds. These data successfully confirm well incorporation and immobilization of ionic liquid groups in the material network.

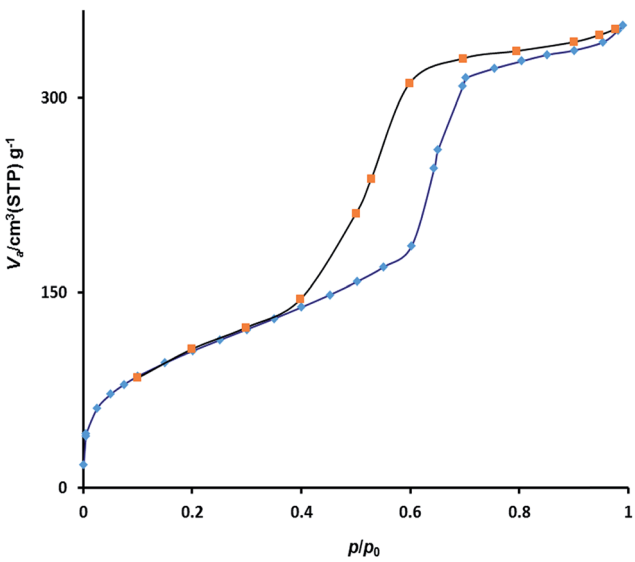

Fig. 3 The nitrogen adsorption–desorption isotherms of Ni@IL-OMO nanocatalyst.

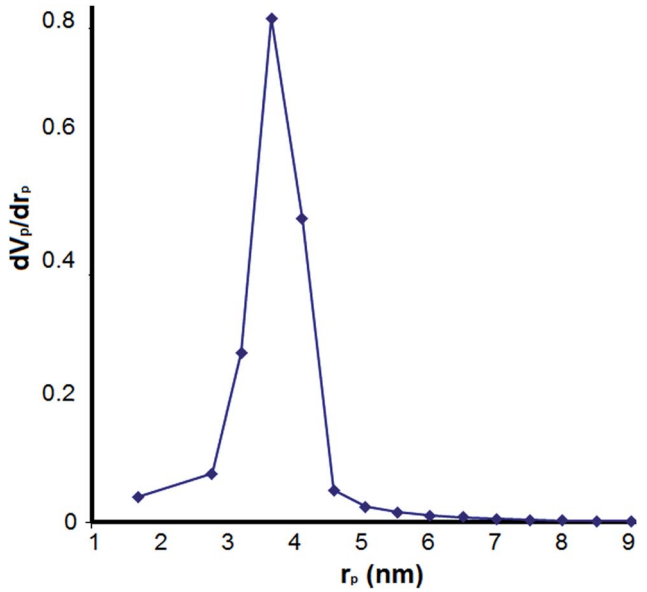

Fig. 4 The BJH pore size distribution isotherm of Ni@IL-OMO nanocatalyst.

TEM image of the nickel-containing IL-OMO was performed to study mesoporosity of the material (Fig. 2). This image showed a hexagonally ordered mesoporous structure with high regularity in the framework for the material. This is characteristic of SBA-15-type materials and confirms high mesoporosity and structure order of the material.

The nitrogen adsorption–desorption analysis showed a type IV isotherm with H1 hysteresis loop (Fig. 3). According to this analysis, the BET surface area and pore volume were, respectively, 565 $m^2\ g^{-1}$ and 0.91 $cm^3\ g^{-1}$. The BJH pore size distribution isotherm of the catalyst illustrated a sharp peak centered at mean pore diameter of 7.5 nanometer (Fig. 4). These results

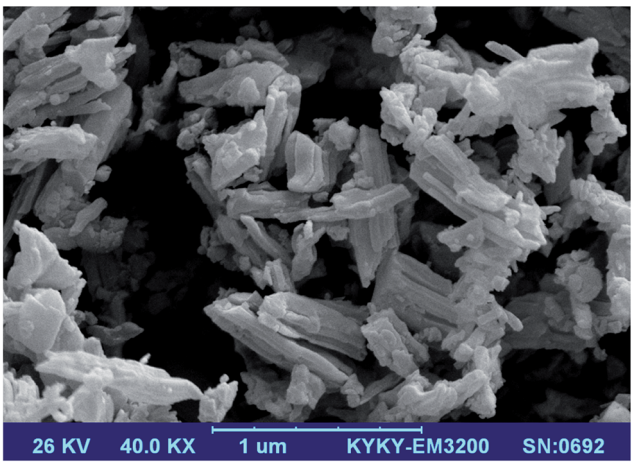

Fig. 5 SEM image of Ni@IL-OMO nanocatalyst.

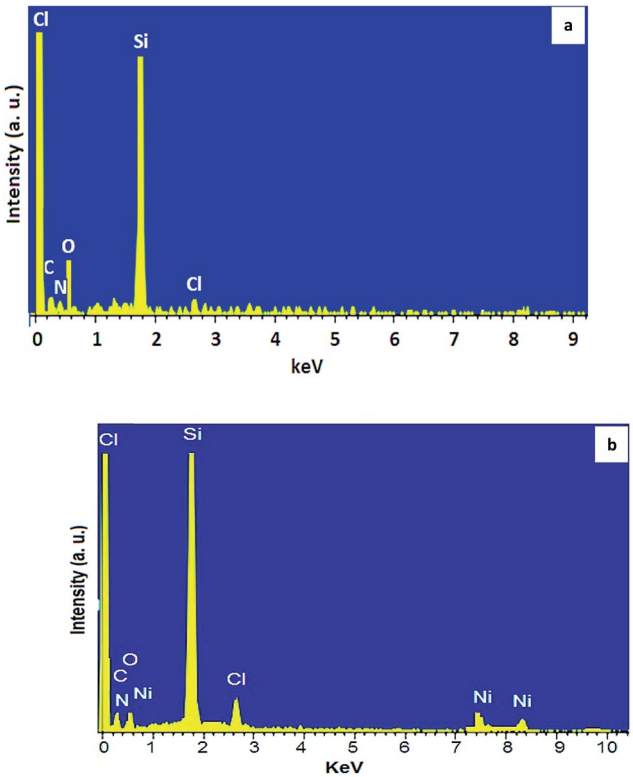

Fig. 6 Energy-dispersive X-ray (EDX) spectrum of (a) IL-OMO and (b) Ni@IL-OMO nanomaterials.

are in good agreement with TEM image and confirm the presence of well-ordered mesostructure for the material.

The SEM image of the Ni@IL-OMO nanocatalyst also showed the presence of particles with uniform morphology and size (Fig. 5) that is an advantage of the material especially in the catalytic and adsorption processes.

The high stability and successful immobilization of ionic liquid groups and Ni-complex were next confirmed by energy-dispersive X-ray (EDX) spectrum (Fig. 6). Before nickel immobilization, the signals of oxygen, silicon, nitrogen, chlorine and carbon were observed (Fig. 6a). While for Ni@IL-OMO (Fig. 6b), the signal of Ni was also seen confirming successful incorporation and/or immobilization of ionic liquid and nickel complex moieties into/onto material framework.

The loading of nickel was calculated using Ni-content obtained from inductively coupled plasma/optical emission spectroscopy (ICP-OES) and also EDX analysis. The result of these two techniques were in good agreement with each other and showed a loading of 0.6 mmol g^{-1} (3.5% wt) for nickel.

After characterization, the catalytic application of Ni@IL-OMO nanocatalyst was investigated in the one-pot Hantzsch condensation of benzaldehyde, ammonium acetate, ethylacetoacetate and dimedone as a test model. The effect of several parameters such as temperature, solvent, and catalyst loading was studied to obtain optimal conditions (Table 1). The study showed that in the absence of catalyst only a trace amount of product was obtained, while in the presence of 0.2 and 0.35 mol% of catalyst, respectively, low to moderate yield was delivered (Table 1, entries 1–3). Interestingly, using 0.5 mol% of Ni@IL-OMO at 70 °C an excellent yield of corresponding Hantzsch product was obtained at very short reaction time (Table 1, entry 4). The solvent effect also illustrated that in toluene low yield, in EtOH and DMF moderate yield, while under solvent-free media excellent yield was achieved under the same reaction conditions (Table 1, entry 4 *versus* entries 5–7). It is also important to note that at 25 and 50 °C low to moderate conversion whereas at 70 °C excellent conversion of starting material were obtained (Table 1, entry 4 *versus* entries 8 and 9). To show the neat effect of supported nickel species in the catalytic process, the efficiency of Ni-free IL-OMO nanomaterial was next studied and the result compared with that of Ni@IL-OMO (Table 1, entry 4 *versus* entry 10). Interestingly, the latter case yielded only 18% of desired product indicating the main catalytic process is affected by supported nickel species. According to these results, the use of 0.5 mol% Ni@IL-OMO nanocatalyst under solvent-free media at 70 °C were selected as optimum conditions.

In the next stage the efficiency of the present catalyst was studied in the Hantzsch condensation of different aldehydes with ammonium acetate, dimedone and ethyl/methylacetoacetate (Table 2).

This demonstrated that the Ni@IL-OMO can convert aromatic aldehydes containing both electron donating and electron-withdrawing substituents to corresponding Hantzsch products under the same conditions and short times. The aliphatic aldehydes such as isobutylaldehyde also delivered corresponding adduct in good yield. These results successfully confirm potent efficiency of the present catalyst for the production of different polyhydroquinoline derivatives applicable in pharmacology and medical sciences.

The recoverability and reusability of the catalyst were then studied to show its stability under applied conditions (Fig. 7). For this, after reaction was completed, hot ethanol was added to the reaction vessel and obtained mixture was centrifuged to precipitation of catalyst. The supernatant solution was removed and the catalyst was recovered and reused in the next run under

Table 1 Effect of temperature, type of catalyst, catalyst loading and solvent in the Hantzsch reaction[a]

Entry	Catalyst	Catalyst loading (mol%)	Temperature (°C)	Solvent	Yield[b] (%)
1	No catalyst	—	70	—	<5
2	Ni@IL-OMO	0.2	70	—	25
3	Ni@IL-OMO	0.35	70	—	55
4	Ni@IL-OMO	0.5	70	—	96
5	Ni@IL-OMO	0.5	70	EtOH	68
6	Ni@IL-OMO	0.5	70	DMF	44
7	Ni@IL-OMO	0.5	70	Toluene	23
8	Ni@IL-OMO	0.5	50	—	55
9	Ni@IL-OMO	0.5	25	—	20
10	IL-OMO	—[c]	70	—	18

[a] Conditions: benzaldehyde (1 mmol), dimedone (1 mmol), ethylacetoacetate (1 mmol) and ammonium acetate (1.5 mmol), 15 min. [b] Isolated yields. [c] The same mg as Ni@IL-OMO was used.

Table 2 Preparation of polyhydroquinolines in the presence of Ni@IL-OMO catalyst under solvent free conditions[a]

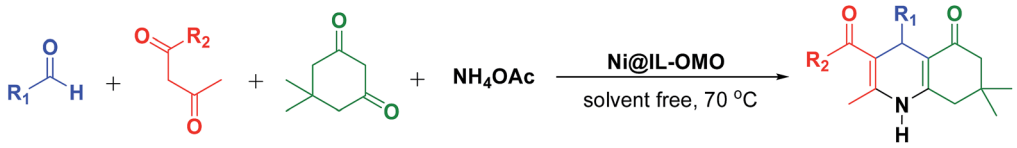

Entry	R_1	R_2	Product	Time (min)	Yield[b] (%)	Mp (°C)
1	C_6H_5	OEt	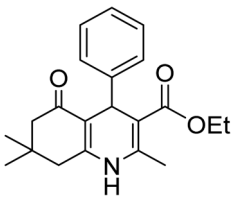	15	96	202–204
2	2-$CH_3C_6H_5$	OEt	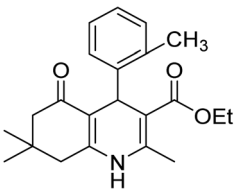	20	95	205–208
3	4-$CH_3OC_6H_5$	OMe	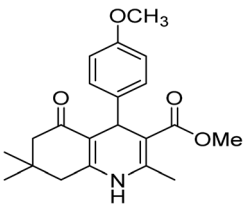	15	95	260–261
4	3-$NO_2C_6H_5$	OMe	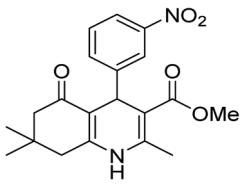	10	92	235–237
5	2-ClC_6H_5	OMe	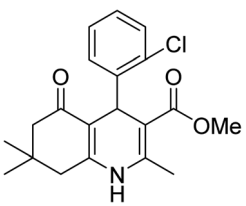	20	86	212–214
6	$(CH_3)_2CH$	OMe	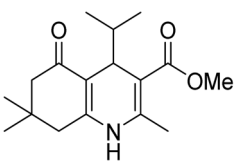	25	72	200–202

[a] Conditions: aldehyde (1 mmol), dimedone (1 mmol), methyl/ethylacetoacetate (1 mmol), ammonium acetate (1.5 mmol) and catalyst (0.5 mol%).
[b] Isolated yields.

the same conditions as the first run. The result showed that this could be recovered and reused at least 9 times without significant decrease in its efficiency.

To illustrate whether the catalyst operates in a homogeneous or heterogeneous manner, in the next study a hot filtration test was performed in the reaction of benzaldehyde, dimedone, ethylacetoacetate and ammonium acetate. For this, after about 40% completion of the reaction, hot ethanol was added and the obtained mixture was hotly filtered. Then the solvent of filtrate was removed and the reaction of residue was allowed to

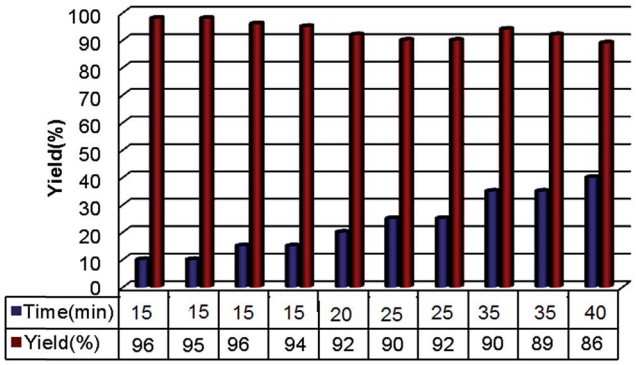

Fig. 7 Reusability of Ni@IL-OMO nanocatalyst in the Hantzsch reaction.

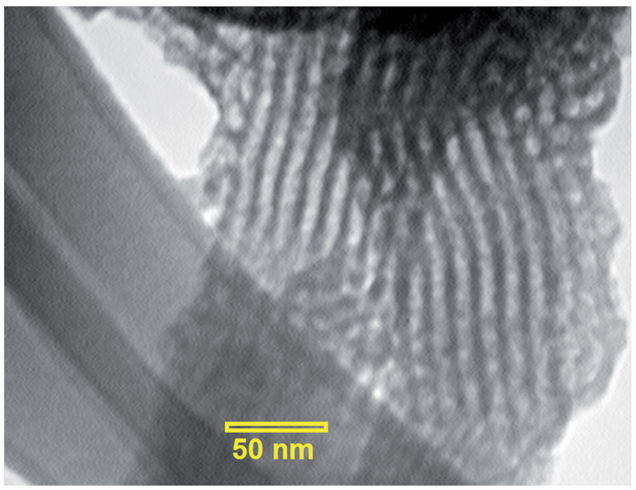

Fig. 8 TEM image of the recovered Ni@IL-OMO nanocatalyst in the Hantzsch reaction.

Table 3 A comparison study between our designed catalyst and recently reported heterogeneous catalytic systems on the Hantzsch reaction

Entry	Catalyst	Conditions	Recycling times	References
1	SnO_2 nanoparticle	SnO_2 (1 mol%) C_2H_5OH, r.t.	4	52
2	PPA–SiO_2[a]	Solvent-free (1.5 mol%), 80 °C	2	53
3	Ni^0-nanoparticle	Solvent free, 25 mg, r.t.	3	44
4	FeF_3	FeF_3 (5 mol%), EtOH, 75–80 °C	4	54
5	TiO_2 nanoparticle	TiO_2 NPs (10 mol%) EtOH, reflux	5	55
6	ZnO nanoparticle	ZnO NPs (5 mol%) solvent-free, 60 °C	2	38
7	Ni@IL-OMO	Ni@IL-OMO (0.5 mol%), solvent free, 70 °C	9	This work

[a] PPA–SiO_2: Silica gel-supported polyphosphoric acid.

continue under optimized conditions. Interestingly, after 2 h a conversion of only about 5% was observed. The atomic adsorption of the filtrate also showed that the amount of nickel species in the solution is lower than 1 ppm. These observations successfully confirm high stability of the supported Ni-catalyst under applied conditions and prove it works in a heterogeneous pathway. The TEM image of the recovered catalyst also showed a well-ordered mesostructure with two dimensional symmetry the same as its fresh parent (Fig. 8) indicating high stability of material structure during reaction process.

In the next, a comparison study was performed between our designed catalyst and recently reported heterogeneous catalytic systems on the Hantzsch reaction (Table 3). The result showed that the present catalytic system was better and/or comparable with those of previous works. Especially, our work were accomplished under solvent free media under moderate conditions and the catalyst was more recoverable than previous catalysts indicating high efficiency of ionic liquid based material for powerful immobilization of active nickel centers.

4. Conclusion

In summary, for the first time a new ionic liquid based mesoporous organosilica supported nickel complex (Ni@IL-OMO) was prepared, characterized and used in the Hantzsch reaction. The TEM and nitrogen-sorption analyses successfully confirmed the presence of a uniform ordered mesostructure for this catalyst. The IR and EDX spectroscopies also showed the well incorporation of ionic liquid and nickel moieties in the material network. This novel nanocatalyst demonstrated excellent performance in the preparation of different derivatives of polyhydroquinolines through Hantzsch reaction. The Ni@IL-OMO was recovered at least nine times with keeping its efficiency and stability under applied reaction conditions. Other advantages of the present study were low loading and easy recoverability of the catalyst, solvent-free conditions, easy work-up and low reaction time. Accordingly, some applications of this catalyst in other organic processes are underway in our laboratory.

Conflicts of interest

There are no conflicts to declare.

Acknowledgements

The authors thank the Yasouj University and the Iran National Science Foundation (INSF) for supporting this work.

References

1 A. P. Wight and M. E. Davis, *Chem. Rev.*, 2002, **102**, 3589–3614.
2 A. Stein, *Adv. Mater.*, 2003, **15**, 763–775.
3 (*a*) K. K. Sharma and T. Asefa, *Angew. Chem., Int. Ed.*, 2007, **46**, 2879–2882; (*b*) K. K. Sharma, R. P. Buckley and T. Asefa, *Langmuir*, 2008, **24**, 14306–14320.

4 (*a*) K. K. Sharma, A. Anan, R. P. Buckley, W. Ouellette and T. Asefa, *J. Am. Chem. Soc.*, 2008, **130**, 218–228; (*b*) A. Corma, *Chem. Rev.*, 1997, **97**, 2373–2419.
5 (*a*) A. Sayari and S. Hamoudi, *Chem. Mater.*, 2001, **13**, 3151–3168; (*b*) C. Li, *Catal. Rev.: Sci. Eng.*, 2004, **46**, 419–492.
6 R. Corriu, A. Mehdi and C. Reye, *J. Organomet. Chem.*, 2004, **689**, 4437–4450.
7 (*a*) P. Van Der Voort, D. Esquivel, E. D. Canck, F. Goethals, I. V. Driessche and F. J. Romero-Salguero, *Chem. Soc. Rev.*, 2013, **42**, 3913–3955; (*b*) U. Díaz, D. Brunel and A. Corma, *Chem. Soc. Rev.*, 2013, **42**, 4083–4097.
8 (*a*) S. E. l. Hankari, B. Motos-Pérez, P. Hesemann, A. Bouhaouss and J. J. E. Moreau, *Chem. Commun.*, 2011, **47**, 6704–6706; (*b*) M. Waki, N. Mizoshita, T. Tani and S. Inagaki, *Angew. Chem., Int. Ed.*, 2011, **50**, 11667–11671.
9 (*a*) F. Hoffmann, M. Cornelius, J. Morell and M. Fröba, *Angew. Chem., Int. Ed.*, 2006, **45**, 3216–3251; (*b*) M. Jaroniec, *Nature*, 2006, **442**, 638–640.
10 D. M. Ford, E. E. Simanek and D. F. Shantz, *Nanotechnology*, 2005, **16**, S458–S475.
11 S. Fujita and S. Inagaki, *Chem. Mater.*, 2008, **20**, 891–908.
12 (*a*) B. Hatton, K. Landskron, W. Whitnall, D. Perovic and G. A. Ozin, *Acc. Chem. Res.*, 2005, **38**, 305–312; (*b*) F. Hoffmann and M. Fröba, *Chem. Soc. Rev.*, 2011, **40**, 608–620.
13 (*a*) N. Mizoshita, T. Tani and S. Inagaki, *Chem. Soc. Rev.*, 2011, **40**, 789–800; (*b*) H. S. Xia, C. H. Zhou, D. S. Tong and C. X. Lin, *J. Porous Mater.*, 2010, **17**, 225–252.
14 F. Hoffmann and M. Fröba, *Supramol. Chem. Org.-Inorg. Hybrid Mater.*, 2010, 39–102.
15 (*a*) G. Dubois, C. Reye, R. J. P. Corriu, S. Brandes, F. Denat and R. Guilard, *Angew. Chem., Int. Ed.*, 2001, **40**, 1087–1090; (*b*) E. Y. Jeong, M. B. Ansari and S. E. Park, *ACS Catal.*, 2011, **1**, 855–863.
16 R. J. P. Corriu, E. Lancelle-Beltran, A. Mehdi, C. Reye, S. Brandes and R. Guilard, *Chem. Mater.*, 2003, **15**, 3152–3160.
17 (*a*) A. Corma, D. Das, H. Garcia and A. Leyva, *J. Catal.*, 2005, **229**, 322–331; (*b*) J. L. Huang, F. X. Zhu, W. H. He, F. Zhang, W. Wang and H. X. Li, *J. Am. Chem. Soc.*, 2010, **132**, 1492–1493; (*c*) C. M. Kang, J. L. Huang, W. H. He and F. Zhang, *J. Organomet. Chem.*, 2010, **695**, 120–127.
18 F. Zhang, C. M. Kang, Y. Y. Wei and H. X. Li, *Adv. Funct. Mater.*, 2011, **21**, 3189–3197.
19 Y. Yang, Y. Zhang, S. J. Hao and Q. B. Kan, *J. Colloid Interface Sci.*, 2011, **362**, 157–163.
20 T. M. Zhang, C. G. Gao, H. Q. Yang and Y. X. Zhao, *J. Porous Mater.*, 2010, **17**, 643–649.
21 B. Karimi, D. Elhamifar, J. H. Clark and A. J. Hunt, *Chem.–Eur. J.*, 2010, **16**, 8047–8053.
22 B. Karimi, D. Elhamifar, J. H. Clark and A. J. Hunt, *Org. Biomol. Chem.*, 2011, **9**, 7420–7426.
23 (*a*) B. Karimi, D. Elhamifar, O. Yari, M. Khorasani, H. Vali, J. H. Clark and A. J. Hunt, *Chem.–Eur. J.*, 2012, **18**, 13520–13530; (*b*) D. Elhamifar, B. Karimi, J. Rastegar and M. H. Banakar, *ChemCatChem*, 2013, **5**, 2218–2224.
24 D. Elhamifar, F. Hosseinpoor, B. Karimi and S. Hajati, *Microporous Mesoporous Mater.*, 2015, **204**, 269–275.
25 (*a*) E. Ulli and J. Kuthan, *Chem. Rev.*, 1972, **72**, 1–42; (*b*) S. M. David and A. I. Meyers, *Chem. Rev.*, 1982, **82**, 223–243.
26 (*a*) T. Godfraid, R. Miller and M. Wibo, *Pharmacol. Rev.*, 1986, **38**, 321–416; (*b*) P. P. Mager, R. A. Coburn, A. J. Solo, D. J. Triggle and H. Rothe, *Drug Discovery Today*, 1992, **8**, 273–289.
27 F. Bossert, H. Meyer and E. Wehinger, *Angew. Chem., Int. Ed.*, 1981, **20**, 762–769.
28 (*a*) G. Roma, M. D. Braccio, G. Grossi and M. Chia, *Eur. J. Med. Chem.*, 2000, **35**, 1021–1035; (*b*) R. Leon, C. de los Rios, J. Marco-Contelles, O. Huertas, X. Barril, F. J. Luque, M. G. Lopez, A. G. Garcia and M. Villarroya, *Bioorg. Med. Chem.*, 2008, **16**, 7759–7769.
29 G. Sabitha, G. S. K. K. Reddy, C. S. Reddy and J. S. Yadav, *Tetrahedron Lett.*, 2003, **44**, 4129–4131.
30 M. Hong, C. Cai and W. B. Yi, *J. Fluorine Chem.*, 2010, **131**, 111–114.
31 L. M. Wang, J. Sheng, L. Zhang, J. W. Han, Z. Y. Fan, H. Tian and C. T. Qian, *Tetrahedron*, 2005, **61**, 1539–1543.
32 C. S. Reddy and M. Raghu, *Chin. Chem. Lett.*, 2008, **19**, 775–779.
33 N. Tewari, N. Dwivedi and R. P. Tripathi, *Tetrahedron Lett.*, 2004, **45**, 9011–9014.
34 S. J. Ji, Z. Q. Jiang, J. Lu and T. P. Loh, *Synlett*, 2004, 831–838.
35 R. Sridhar and P. T. Perumal, *Tetrahedron*, 2005, **61**, 2465–2470.
36 J. S. Yoo, T. J. Laughlin, J. J. Krob and R. S. Mohan, *Tetrahedron Lett.*, 2015, **56**, 4060–4062.
37 R. Pagadala, S. Maddila, V. D. B. C. Dasireddy and S. B. Jonnalagadda, *Catal. Commun.*, 2014, **45**, 148–152.
38 F. Tamaddon and S. Moradi, *J. Mol. Catal. A: Chem.*, 2013, **370**, 117–122.
39 J. Safari, S. H. Banitaba and S. D. Khalili, *J. Mol. Catal. A: Chem.*, 2011, **335**, 46–50.
40 E. Rafiee, S. Eavani, S. Rashidzadeh and M. Joshaghani, *Inorg. Chim. Acta*, 2009, **362**, 3555–3562.
41 M. Nasr-Esfahani, S. J. Hoseini, M. a. Montazerozohori, R. Mehrabi and H. Nasrabadi, *J. Mol. Catal. A: Chem.*, 2014, **382**, 99–105.
42 M. Kaur, S. Sharma and P. M. S. Bedi, *Chin. J. Catal.*, 2015, **36**, 520–549.
43 T. R. R. Naik and S. A. Shivashankar, *Tetrahedron Lett.*, 2016, **57**, 4046–4049.
44 L. Saikia, D. Dutta and D. K. Dutta, *Catal. Commun.*, 2012, **19**, 1–4.
45 M. Maheswara, V. Siddaiah, Y. K. Rao, Y.-M. Tzeng and C. Sridhar, *J. Mol. Catal. A: Chem.*, 2006, **260**, 179–180.
46 H. Adibi, H. A. Samimi and M. Beygzadeh, *Catal. Commun.*, 2007, **8**, 2119–2124.
47 S. B. Sapkal, K. F. Shelke, B. B. Shingate and M. S. Shingare, *Tetrahedron Lett.*, 2009, **50**, 1754–1756.
48 P. Gholamzadeh, G. Mohammadi Ziarani, N. Lashgari, A. Badiei and P. Asadiatouei, *J. Mol. Cat. A: Chem.*, 2014, **391**, 208–222.

49 H. Zhao, N. Yu, J. Wang, D. Zhuang, Y. Ding, R. Tan and D. Yin, *Microporous Mesoporous Mater.*, 2009, **122**, 240–246.
50 (*a*) D. Elhamifar and A. Shábani, *Chem.–Eur. J.*, 2014, **20**, 3212–3217; (*b*) D. Elhamifar, M. Nasr-Esfahani, B. Karimi, R. Moshkelgosha and A. Shábani, *ChemCatChem*, 2014, **6**, 2593–2599; (*c*) D. Elhamifar, S. Kazempoor and B. Karimi, *Catal. Sci. Technol.*, 2016, **6**, 4318–4326.
51 J. G. Groissant, X. Cattoën, M. W. C. Man, J.-O. Durand and N. M. Khashab, *Nanoscale*, 2015, **7**, 20318–20334.
52 S. M. Vahdat, F. Chekin, M. Hatami, M. Khavarpour, S. Baghery and Z. Roshan-Kouhi, *Chin. J. Catal.*, 2013, **34**, 758–763.
53 A. Khojastehnezhad, F. Moeinpour and A. Davoodnia, *Chin. Chem. Lett.*, 2011, **22**, 807–810.
54 R. Surasani, D. Kalita, A. D. Rao, K. Yarbagi and K. B. Chandrasekhar, *J. Fluorine Chem.*, 2012, **135**, 91–96.
55 M. Tajbakhsh, E. Alaee, H. Alinezhad, M. Khanian, F. Jahani, S. Khaksar, P. Rezaee and M. Tajbakhsh, *Chin. J. Catal.*, 2012, **33**, 1517–1522.